

D 555
I-69



July, 11-16, 1999, Warsaw, **Poland**

XXIV

**I
C
P
I
G**

International

Conference on

Phenomena in

Ionized

Gases

Proceedings

Contributed Papers

Wednesday, July 14

VOL. III

On Numerical And Laboratory Simulations Of Magnetic Nova Star Burst

S.A.Nikitin¹, A.G.Ponomarenko², Yu.P.Zakharov², G.I.Dudnikova³, V.A.Vshivkov³,
V.M.Antonov², V.G.Posukh², A.V.Melekhov², I.F.Shaikhislamov², V.N.Snytnikov⁴, P.D.Vobly¹

1-Budker Institute of Nuclear Physics SB RAS, Novosibirsk 630090;

2-Institute of Laser Physics SB RAS, Novosibirsk 630090;

3-Institute of Computational Technologies SB RAS, Novosibirsk 630090;

4- Borekov Institute of Catalysis SB RAS, Novosibirsk 630090

Introduction

According to the hypothesis [1], an asymmetrical character of the shell expansion observed at many Novae may be associated with influence of an inherent star magnetic field. Magnetization of Novas' cores reaches the field value $B \sim 10^6 - 10^8$ gauss [2]. Typically, a magneto-dipole energy of a Nova ($10^{38} - 10^{42}$ ergs) is much less than a kinetic energy of an exploding envelope ($10^{44} - 10^{46}$ ergs). By this reason the conventional hydrodynamic models of point-like explosion with a spherical outward-directed shock wave do not consider effects of the star magnetic field on plasma movement [3]. The approach has been developed in [4] to account for a certain spatial scale of formation of initial perturbations. In this case the magnetic field can play a "work body" role with pronounced anisotropic properties and effect upon an interaction of the shell with the near-star media. Mentioned peculiarities have been studied in [4] using the numerical model based on the kinetic-hydrodynamic description of plasma dynamics. The possibility is of interest to perform a laboratory simulation of a magnetic star's shell outburst at the KI-1 facility (ILP SB RAS, Novosibirsk) by the laser-produced-plasma methods. Formerly the braking of supernova shells in the interstellar magnetic field was simulated there [5].

1. Physical model

In the approximation of the star by a gravitating magnetized sphere from incompressible fluid the gravitation may exert influence only upon a total scale (not a structure) of initial perturbations ($10^2 - 10^3$ of the star radius R) by compression action of the exploding envelope [4]. This allows to do not include the star gravitation into the model under our consideration. A role of magnetic field is described by two parameters. First of them governs the scale of perturbations associated with magnetic field compression and equals to a ratio of the shell's kinetic energy (E) to the magneto-dipole energy of Nova star in external space: $\alpha = 12E/(B^2 R^3) \sim 10^2 - 10^8$. Second parameter is the Mach-Alfven number determined by a ratio of the shell velocity (V) to Alfven velocity (V_A) in plasma medium in vicinity of the star: $M_A = V/V_A$. Due to a high density of the star wind by the early burst when the surface temperature reaches $\sim 10^8$ K with the surface density $\sim 10^4$ g/cm³ [6], the plasma shell movement after the explosion may be of super-Alfven character at distances of the order of R from the star: $M_A \gg 1$. That is the

magneto-laminar mechanism [7] of interaction between expanding plasma flows and a background dominates. Given conditions determine parameters of the physical model [4], which includes an uniformly magnetized and perfectly conducting sphere, a thin exploding envelope around it, and a rarefied ionized gas in surrounding space.

2. Numerical simulation of a Super-Alfven expansion of magnetic Nova shell

The numerical model of plasma is based on the system of equations of the hybrid type [8]. It gives an opportunity to consider a complicated multi-flow motion of particles in plasma at $M_A \gg 1$. At the beginning ($t=0$), there is an immobile (cold) background plasma of a homogeneous concentration in a cylindrical region with a dipole magnetic field. Into the central spherical region of radius R , where the magnetic field remains uniform and constant at all times, the external plasma does not penetrate with elastic reflections of ions at the spherical core surface. This boundary is spaced at $\Delta R \ll R$ of the spherical envelope which consists of the ions with the total energy E . At $t=0$ the radial velocities of the envelope ions are distributed in the interval $[-V, V]$ from the law providing auto-modeling expansion in free space. In one of the variants the core field is $2.6 \cdot 10^7$ gauss; the ions velocity is $V = 3 \cdot 10^8$ cm/s; $E = 10^{43}$ ergs and $\alpha \sim 10^2$. Nearby the core surface the hydrogen background density is $7 \cdot 10^{23}$ cm⁻³, the Mach-Alfven number $M_A = 5$. Some preliminary results of simulation [4] are presented in Fig.1-2, where the distribution of the combined concentration of the envelope and the background as the isodensity lines, and also the perturbed magnetic lines of force are shown at the moment $\tau = t \cdot V / \Delta R = 4$ ($\Delta R = 0.2R$). The symmetry and the structure manifested are similar to the morphological features observed under development of outbursts of those Novae whose shells took an ellipse-like form and had the characteristic structure as polar fragments and equatorial belts [1]. With decreasing the number M_A from 5 down to 2.5 at $\alpha \approx \text{const}$, the envelope-background interaction efficiency drastically drops and a picture of expansion becomes close to a spherically homogeneous one. The effect of the magnetic perturbations of quadrupole symmetry (see Fig.2) is disappeared as well as its associated magnetic lines reconnection and the generation of fast waves in directions making 45° with the dipole axis. The similar modifications also take a place with increasing the

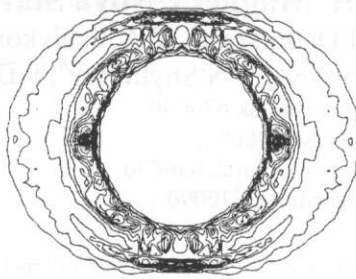


Fig.1. Isodensity lines at $M_A=5$, $\alpha=10^2$, $\tau=4$ (magnetic axis is horizontal; the star core looks as a light circle).

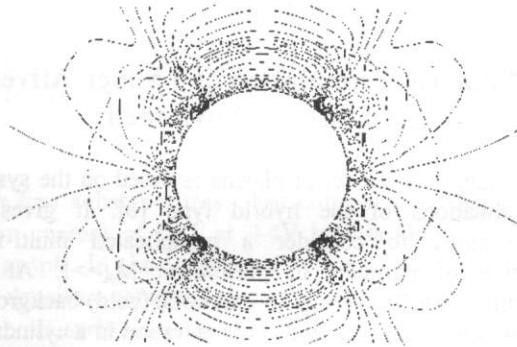


Fig.2. Perturbed magnetic field (an ellipse-like counter shows the outer boundary of expanding shell).

energetic parameter by three orders of magnitude up to the level $\alpha \sim 10^5$ at the fixed number $M_A=5$.

3. On laser-produced-plasma experiments with magnetized spherical target

By now we have made first samples of the target in the form of the uniformly magnetized neodymium-iron-boron balls of $\varnothing 8$ and $\varnothing 16$ mm. To impart high conductivity features to them, the magnetic cores are covered by the 1mm copper layer. The target outside is the caprolactam ($H_{11}C_6ON$) envelope of the 1mm thickness. The core is magnetized up to the field level about of 7 kilogauss. Preliminary results have been obtained in the laser-produced-plasma experiment with the flat caprolactam target irradiated by the 100 nanosecond and 100 Joule pulse of the CO_2 laser with the focal spot sizes $1 \times 1.4 \text{ cm}^2$. Fig.3 shows the typical oscillogram of the current density at the cylindrical Langmuir probe removed at the distance 20.5 cm from the target. The formed flow of ions is characterized by a steep forward front, having the speed of $V=(4 \div 5) \cdot 10^7 \text{ cm/s}$, and the slower main plasma. Total number of ions in the plasma expanding into a cone with an angle of spreading of 90° is about of $(1 \div 3) \cdot 10^{16}$, a mean charge number $Z=2.7$ and the total kinetic energy about of 10 Joules (the magnetic energy of the $\varnothing 8$ mm core is about of 0.1 Joules, or $\alpha \sim 10^2$).

In the experiment on quasi-spherical irradiation (using two laser beams) of the magnetized target in vacuum we intend to study diamagnetic features of the exploding plasma envelope [4]. In the variant with placement of the target into a gas medium we assume to use an

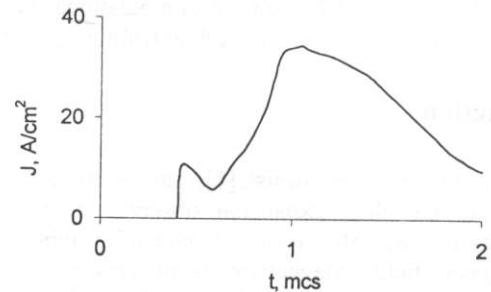


Fig.3. The typical oscillogram of the current density $J_i = Z e n_i V_i$ at the Langmuir probe placed at 20.5cm from the target with the focal spot sizes $1 \times 1.4 \text{ cm}^2$.

inherent VUV radiation of laser-produced plasma to create a background "cold" plasma satisfied to conditions of super-Alfven expansion of the envelope. Necessary ion concentration of a background $n_i \geq B \cdot M_A^2 / (4\pi m \cdot V^2)$ and $n_i \ll B \cdot \alpha^2 / (8\pi kT)$ may reach the value $n_i = (1 \div 2) \cdot 10^{13} \text{ cm}^{-3}$ for hydrogen plasma at $B=200$ gauss and $M_A \approx 3$ (M_A can be increased if to replace hydrogen by nitrogen).

Conclusions

Calculation results give an indication of emergence of characteristic inhomogeneities in distribution of plasma and field perturbations under super-Alfven expansion of a magnetic Nova's shell in near-star medium. Main features of such a magnetic field-plasma configuration can be simulated in experiments at the KI-1 facility.

Acknowledgements

This work has been supported by the Russian Fund of Basic Researches (N 97-02-18471).

References

- [1] A.A.Bojarchuk & E.R.Mustel: *Astrophys. and Sp. Sc.*, V.6, No. 2, 1970, p.183.
- [2] M.Livio, A.Shankar & J.W.Truran: *Astrophys. J.*, V.330, 1988, p.264.
- [3] B.C.Low: *Astrophys. J.*, V.261, 1982, p.351.
- [4] S.A.Nikitin, V.A.Vshivkov & V.N.Snytnikov: *Computational Technologies*, V.3, No.4, 1998, p.65.
- [5] Yu.P.Zakharov et al: *Laser.Inter.Relat.Plasma.Phen.*, AIP Conf.Proc., 1996, V.369, Pt.I, p.347.
- [6] S.Starrfield, J.W.Truran & W.M.Sparks: *Astrophys.J.*, V.226, 1978, p.186.
- [7] V.P.Bashurin, A.I.Golubev & V.A.Terekhin: *Prikl.Mekh.Tekhn.Fiz.*, v.5, 1983, p.10.
- [8] V.A.Vshivkov, G.I.Dudnikova & Yu.I.Molodov: *Computational Technologies*, V.4, No.10, 1995.

RF PLASMA EMITTER FOR DIAGNOSTIC NEUTRAL BEAM INJECTOR

I.V.Shikhovtsev, G.F.Abrashitov, V.I.Davydenko, P.P.Deichuli, A.A.Ivanov, V.V.Mishagin,
I.I.Averbukh, A.A.Podminogin

Budker Institute of Nuclear Physics, 630090, Novosibirsk, Russia

1. INTRODUCTION.

We developed a neutral beam injector based on RF-discharge plasma source for beam emission spectroscopy in TEXTOR tokamak [1]. The injector was designed to be rated at energy 50 keV, equivalent neutral beam current (for hydrogen) of up to 1A and pulse duration of up to 10s. The developed power supplies for the injector were designed to provide beam modulation at 500Hz frequency. In the ion source, the plasma for the beam extraction is produced by RF plasma emitter. In the paper we describe the experimental results obtained in the RF-discharge plasma emitter studies.

2. ION SOURCE

In the injector ion source (see Fig.1), plasma emitter is produced by an inductively driven RF-discharge with a frequency of about 4.6 MHz. Hydrogen gas is puffed into the ceramic discharge chamber (1) with inner diameter of 103mm and axial length of 90mm through dielectric tubing (2) installed at the copper end flange. The permanent magnets (3), that improve plasma homogeneity at the plasma grid, are located at the end flange. The plasma discharge is exited by 6-turn loop antenna (4). To initiate the discharge we used a triggering electrode installed at the end flange.

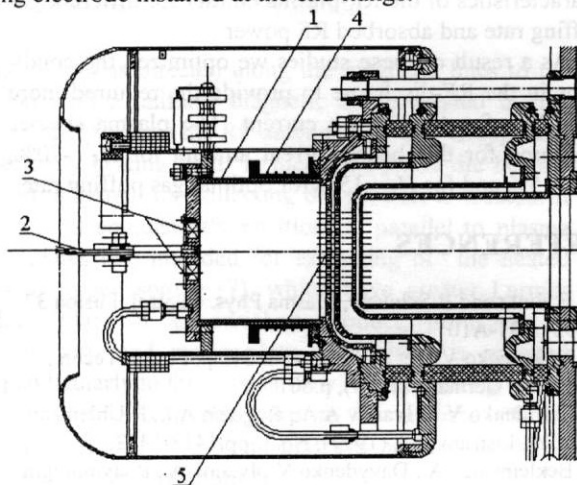


Fig. 1. Ion source layout:

1-ceramic discharge chamber; 2-dielectric tubing for gas puff; 3-permanent magnets; 4-RF coil; 5- grids.

The beam is extracted and accelerated by a four-electrode ion-optics system (5) with the 163 circular apertures each 4mm in diameter [2,3]. Geometry of the elementary cell was optimized to obtain minimal beam divergence [3]. The grids are spherically formed in order to obtain the beam focusing at 4m downstream from

the source. The thickness of the grids was 2mm, 4mm, 4mm, and 2mm for the plasma grid, extracting grid, accelerating grid and grounded grid correspondingly. Initial beam size (~70mm) is defined by the grids diameter.

The Mo-grids of ion-optics system are soldered to copper holders and then fixed to the supports also made of copper. We designed a thermal inertia-type ion optical system with «thick» electrodes whose distinctive feature is that the grids are cooled between pulses by water flowing in the tubes soldered to the supporting flanges [4]. Application of this method of grids cooling, of course, becomes possible if the time-averaged heat loads on the grids are small enough as it is for the given source parameters.

2. EXPERIMENTAL RESULTS

2.1 RF- power dependence of the current density.

Two miniaturized Faraday cups were inserted into the two apertures of IOS. One of those cups was located in the center and another at the periphery of the plasma grid ($r=35\text{mm}$). It was observed that with the increase of RF-power, the current measured in the center beamlet increases faster than that on the periphery. Fig.2 shows the current density measured by the cups as a function of the power consumption of RF generator. The RF power absorbed in the discharge was measured to be about 20-25% of the power consumed by the generator.

We found that to achieve the required $120\text{mA}/\text{cm}^2$ current density of the plasma emitter about 3.5kW of absorbed RF power is required (that corresponds to about 12kW consumed from the grid).

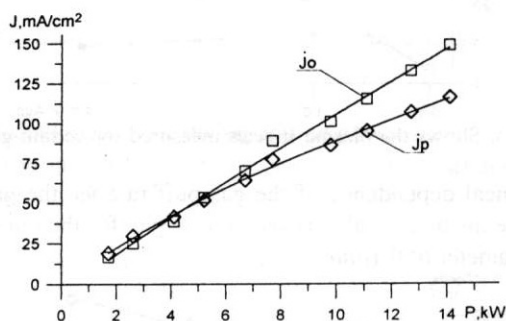


Fig. 2. The current densities measured in the center (j_0) and at the periphery (j_p) vs. the power consumed by the RF-generator.

2.2 Gas pressure dependence of the current density and plasma homogeneity over the emitter.

Gas puffing into the discharge was varied by changing the gas pressure in the gas valve and, alternatively, by changing the diameter of the hole through

which the gas was entered the discharge chamber. The average current density $j_a=(j_o+j_p)/2$ as a function of pressure for the fixed RF power is shown on the Fig.3.

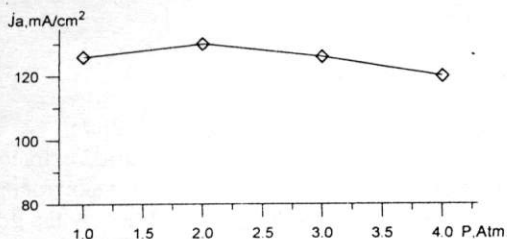


Fig.3. The average current density as a function of pressure in the valve.

For the same conditions relative difference between the measured current $((j_o-j_p)/j_a)$ which characterize homogeneity of plasma emitter is shown on the Fig.4.

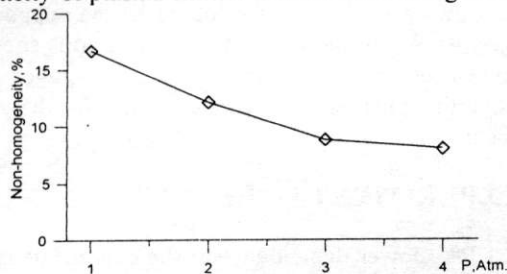


Fig.4. Non-homogeneity of plasma emitter vs. gas pressure in the valve.

2.3 Variation of extracted beam composition with pressure in the valve.

For the certain diameter of the gas inlet hole the plasma species in the discharge (Fig.5) were measured for different gas pressures in the valve.

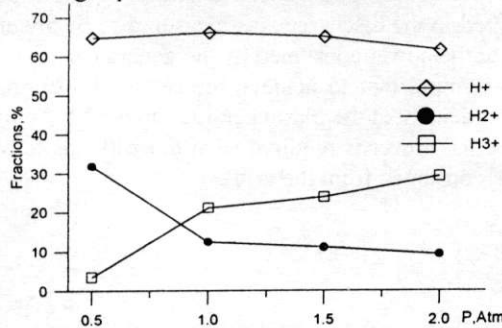


Fig.5. Shows the plasma species measured for certain gas puffing.

Typical dependence of the gas puff rate vs. the gas pressure inside the valve is shown in Fig.6. for the outlet hole diameter of 0.1mm.

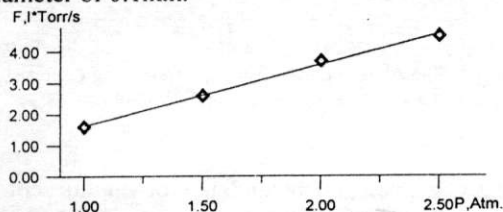


Fig.6 Gas puff rate vs. the gas pressure inside the valve.

2.4 Variation of the plasma composition over the emitter.

Measurements of the beam composition 4m down-

stream from the source indicated the the beam composition is radius dependent.

In the optimal conditions with the extracted current of 2A (averaged current density of 120mA/cm²), the ion beam species were measured on the beam axis to be 74% for H₁⁺, 13% for H₂⁺ and 13% for H₃⁺. On the beam periphery, at radius 2.5cm, the beam species were: H₁⁺ -60%, H₂⁺ -27%, H₃⁺ -13%. The difference of beam species in the center and at periphery leads to different beam profiles (Fig.7) measured by making use of an array of secondary emission detectors and the calorimetric detectors measured at the focal plane of the ion-optical system.

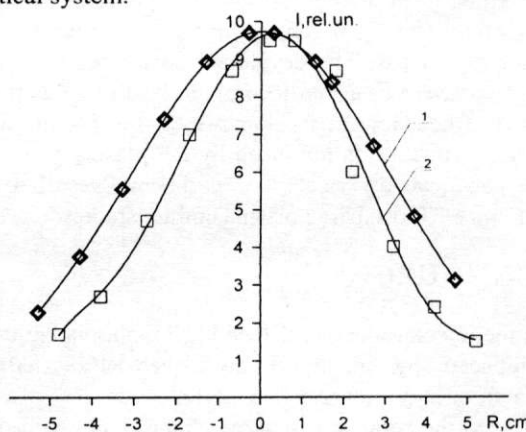


Fig.7 The current density profiles measured by making use of an array of secondary emission detectors (1) and the calorimetric detectors (2).

4. CONCLUSIONS

The main objective of the experiments was to study characteristics of the RF-plasma emitter for different gas puffing rate and absorbed RF power.

As a result of these studies we optimized the conditions in the RF-discharge to provide the required more than 2A of extracted ion current. The plasma species measured for this beam current amount for H₁⁺ -70%, H₂⁺ -15% and for H₃⁺ -15% for optimal gas puffing rate.

REFERENCES

- [1] E.Hintz and B.Schweer, Plasma Phys. Control. Fusion 37 (1995) A87-A101
- [2] Davydenko V.I. et al, Proc. 18th Symp. Fusion Techn., Karlsruhe, Germany (1994), p.601
- [3] Davidenko V.I., Ivanov A.A., Rogozin A.I., R.Uhlemann, Rev. Sci. Instrum., 68, (1997), No.3, pp.1418-1422.
- [4] Beklemishev A., Davydenko V., Ivanov A., Podyminogin A., Rev.Sci.Instrum., 69,(1998), No. 5, pp.2007-2012.